Cardiovascular Research (2012) **95**, 460–468
doi:10.1093/cvr/cvs218

Sodium current deficit and arrhythmogenesis in a murine model of plakophilin-2 haploinsufficiency

Marina Cerrone[1†], Maartje Noorman[2,3†], Xianming Lin[1], Halina Chkourko[1], Feng-Xia Liang[4], Roel van der Nagel[2], Thomas Hund[5,6,7], Walter Birchmeier[8], Peter Mohler[5,6,7], Toon A. van Veen[2], Harold V. van Rijen[2], and Mario Delmar[1*]

[1]Division of Cardiology, New York University School of Medicine, New York, NY, USA; [2]Department of Medical Physiology, University Medical Center Utrecht, The Netherlands; [3]Interuniversity Cardiology Institute of the Netherlands, New York University School of Medicine, 522 First Avenue. Smilow 805, New York, NY 10016, USA; [4]The Office of Collaborative Science Microscopy Core, New York University School of Medicine, New York, NY, USA; [5]Dorothy M. Davis Heart and Lung Research Institute, The Ohio State University Medical Center, Columbus, OH, USA; [6]Division of Cardiovascular Medicine, Department of Internal Medicine, The Ohio State University Medical Center, Columbus, OH, USA; [7]Department of Physiology and Cell Biology, The Ohio State University Medical Center, Columbus, OH, USA; and [8]Max Delbrück Center for Molecular Medicine (MDC), Berlin-Buch, Germany

Received 12 April 2012; revised 7 June 2012; accepted 28 June 2012; online publish-ahead-of-print 3 July 2012

Time for primary review: 25 days

Aims The shRNA-mediated loss of expression of the desmosomal protein plakophilin-2 leads to sodium current (I_{Na}) dysfunction. Whether *pkp2* gene haploinsufficiency leads to I_{Na} deficit *in vivo* remains undefined. Mutations in *pkp2* are detected in arrhythmogenic right ventricular cardiomyopathy (ARVC). Ventricular fibrillation and sudden death often occur in the 'concealed phase' of the disease, prior to overt structural damage. The mechanisms responsible for these arrhythmias remain poorly understood. We sought to characterize the morphology, histology, and ultrastructural features of PKP2-heterozygous-null (PKP2-Hz) murine hearts and explore the relation between PKP2 abundance, I_{Na} function, and cardiac electrical synchrony.

Methods and results Hearts of PKP2-Hz mice were characterized by multiple methods. We observed ultrastructural but not histological or gross anatomical differences in PKP2-Hz hearts compared with wild-type (WT) littermates. Yet, in myocytes, decreased amplitude and a shift in gating and kinetics of I_{Na} were observed. To further unmask I_{Na} deficiency, we exposed myocytes, Langendorff-perfused hearts, and anaesthetized animals to a pharmacological challenge (flecainide). In PKP2-Hz hearts, the extent of flecainide-induced I_{Na} block, impaired ventricular conduction, and altered electrocardiographic parameters were larger than controls. Flecainide provoked ventricular arrhythmias and death in PKP2-Hz animals, but not in the WT.

Conclusions PKP2 haploinsufficiency leads to I_{Na} deficit in murine hearts. Our data support the notion of a cross-talk between desmosome and sodium channel complex. They also suggest that I_{Na} dysfunction may contribute to generation and/or maintenance of arrhythmias in PKP2-deficient hearts. Whether pharmacological challenges could help unveil arrhythmia risk in patients with mutations or variants in PKP2 remains undefined.

Keywords Arrhythmia (mechanisms) • Cell communication • Genetic disorders • Ion channels • Nachannel • Right ventricular • ARVC

1. Introduction

The first descriptions of the intercalated disc defined three structures, all involved in cell–cell communication (desmosomes, adherens junctions, and gap junctions). It is now generally accepted that molecules not involved in forming a physical continuum between neighbouring cells also populate the intercalated disc. Key among them is $Na_v1.5$, the pore-forming subunit of the sodium channel most abundant in the heart. Recent studies have shown that $Na_v1.5$ functionally and physically interacts with other intercalated disc proteins, such as SAP-97,[1] Connexin43 (Cx43),[2,3] and the desmosomal protein plakophilin-2 (PKP2).[3,4] The latter studies further showed that the siRNA-mediated loss of PKP2 expression affects the amplitude and kinetics of the sodium current. These observations, however, were

* Corresponding author. Tel: +1 212 263 9492; fax: +1 212 263 4129, Email: mario.delmar@nyumc.org

† Contributed equally.

limited to studies in isolated cells, where PKP2 expression was acutely disrupted *in vitro*. Whether PKP2 deficiency and, in particular, *pkp2* haploinsufficiency leads to sodium current (I_{Na}) deficit *in vivo*, remains undefined.

The importance of PKP2 in cardiac function is highlighted by the fact that mutations in the *pkp2* gene are found in several cases of arrhythmogenic cardiomyopathy (AC; also known as 'arrhythmogenic right ventricular cardiomyopathy' or 'ARVC'). Of relevance, ventricular fibrillation and sudden death in patients with AC often occur in the 'concealed phase' of the disease, prior to overt structural damage (see ref.[5] for review). The mechanisms responsible for life-threatening arrhythmias in the concealed phase of AC remain unclear. We postulate that sodium channel function is disrupted by PKP2 haploinsufficiency. As such, we propose that sodium channel dysfunction may be a contributing factor to arrhythmogenesis in PKP2-deficient hearts.

Germline knockout of PKP2 in mice leads to embryonic lethality.[6] However, heterozygous animals are viable and live through adulthood. The structural and functional consequences of PKP2 deficiency in the murine heart remain to be defined. In the present study, we conducted a general characterization of the anatomical, histological, and ultra-structural features of the hearts of mice heterozygous null for PKP2 (PKP2-Hz). Our studies revealed that the PKP2-Hz hearts showed ultrastructural, but not histological or gross anatomical differences, when compared with wild-type (WT) littermates. Yet, in myocytes from these structurally normal hearts, a sodium current deficit was observed. Previous studies have shown that the consequences of sodium current deficiency on cardiac electrophysiology can be unmasked by exposure to sodium channel blockers, such as flecainide.[7–12] We therefore exposed isolated myocytes, Langendorff-perfused hearts, and anaesthetized animals with the PKP2-Hz genotype, and their control littermates, to this drug. Our results show that in PKP2-Hz hearts, the extent of flecainide-induced use-dependent I_{Na} block, impaired ventricular conduction, and altered electrocardiographic parameters were larger than in controls. The pharmacological challenge also provoked ventricular arrhythmias and death in PKP2-Hz animals, but not in the WT controls. The possible implications of these findings to the pathophysiology of AC are discussed.

2. Methods

The methods for generation of the PKP2-Hz line and the characterization of homozygous-null animals have been reported before.[6] All experiments were conducted in PKP2-Hz and WT littermate mice, 3–6 months old, both genders. Mice were euthanized with an overdose of anaesthetic (isoflurane >20%) and confirmation of death by cervical dislocation. All procedures were carried out in accordance with New York University guidelines (IACUC Protocol 101101-02 to MD approved on 7 November 2011) for animal use and care and conformed to the *Guide for the Care and Use of Laboratory Animals* published by the US National Institutes of Health (NIH Publication 58-23, revised 1996). Detailed methods in Supplementary material online. Brief descriptions are as follows.

2.1 Myocyte isolation and cell electrophysiology

Adult mouse ventricular myocytes were obtained by enzymatic dissociation following standard procedures. All electrophysiological recordings were conducted in whole-cell configuration. Voltage clamp protocols were applied for determination of peak current–voltage relation, steady-state activation, steady-state inactivation, and recovery from inactivation.[3] For assessing the effect of flecainide on peak sodium current amplitude, voltage clamp steps were applied repetitively every 300 ms. Control recordings (no drug added) were obtained for a total of 50–60 s after patch break. Three minutes after drug addition, voltage clamp was switched back on and voltage clamp protocol reinitiated. The time-dependent peak sodium current amplitude decay curves were fit with bi-exponential functions.

2.2 Epicardial electrical mapping of Langendorff-perfused hearts

Hearts were placed on a Langendorff column and extracellular electrograms recorded using a 247-point terminal electrode (19 × 13 grid, 0.3 mm spacing) placed over both LV and RV.[13–15] Recordings were made during stimulation from the centre of the grid. Measurements were repeated on the same hearts after 5 min of continuous perfusion of a Tyrode solution containing 0.53 μmol/L of flecainide.

2.3 Flecainide challenge and electrocardiographic recording in anesthetized mice

Mice were anaesthetized with isoflurane (5% for induction, then maintained at 1–1.5% in 700 mL O_2/minute via a nose cone), placed on a heating pad, and a single 'standard-lead' electrocardiogram (ECG) recorded through electrodes placed on limbs. After control recording, flecainide was applied in single bolus by intraperitoneal injection and ECG continuously monitored for 20 min (or arrhythmic death).[16]

2.4 Protein identification, immunohistochemistry, histology, electron microscopy, and electron tomography

Experiments were carried out as in previous studies.[17–19] Total murine heart lysate was prepared and equal amounts of protein (25 μg/lane) of each sample separated on SDS–polyacrylamide gels and transferred to nitrocellulose membranes. After first and second antibody incubation, immune reactivity was detected by ECL chemiluminescence.

To detect protein localization by immunofluorescence, hearts were rapidly frozen in liquid nitrogen and stored at −80°C. Hearts were sectioned (thickness: 10 μm) in direction parallel to the long axis of the heart. Samples were exposed to polyclonal antibody against $Na_V1.5$ (1:100)[19] and mouse monoclonal antibody against N-Cadherin (1:800, Sigma, Aldrich), or PKP2 (1:1000, Progen) and visualized by conventional epifluorescence microscopy. To evaluate extent of fibrosis, sections were fixed with 4% paraformaldehyde in PBS, stained with Picrosirius Red, and examined by light microscopy. For electron microscopy, mouse hearts were fixed *in situ* with 4% paraformaldehyde in 0.1 M PBS (pH 7.4); small pieces were cut, rapidly frozen with a high-pressure freezer, and stored under liquid nitrogen with 2% Osmium Tetroxide in acetone. Samples were slowly warmed by using an automated freeze substitution machine, infiltrated with acetone:Embed 812 resin 1:1, then incubated in twice pure Embed 812, and polymerized at 60°C. Thin sections were collected on slotted copper grids. Samples were tilted between −70 and +70° at 1° intervals and electron micrographs recorded at 15 000 to 25

000 fold magnifications. A second tilt series of the same area was collected after manually rotating the specimen support by 90°.

3. Results

3.1 General characterization of the animal model

PKP2-Hz mice and their WT littermates were used for the study. PKP2-Hz animals showed normal size and appearance. No difference in survival was observed when compared with WT littermates. Hearts from PKP2-Hz animals were also normal in appearance and weight (HW/BW = 0.58 ± 0.02; $n = 12$ and 0.62 ± 0.02; $n = 13$ for WT and PKP2-Hz, respectively). Histological examination revealed no evidence of fibrotic infiltrates in PKP2-Hz compared with control (*Figure 1A*). Western blot analysis showed the expected decrease in PKP2 protein abundance, and no differences in abundance of other intercalated disc proteins (Cx43, N-Cadherin, plakoglobin, or $Na_V1.5$; *Figure 1B*). Immunofluorescence studies showed an apparent decrease in intensity of PKP2 signals, which remained localized to the intercalated disc (*Figure 1C*). Similarly, no changes in localization of $Na_V1.5$, Cx43, plakoglobin, or N-Cadherin were observed at this level of resolution (*Figure 1D* and Supplementary material online, *Figures S1 and S2*). However, ultrastructural analysis of sections that ran parallel to fibre direction showed that desmosomes were sporadic or absent, the dimension of the intercellular space between structures was non-uniform and expanded in some areas, particularly at the crests of the area composita (*Figure 2*, left panels). These observations were consistent with those from other models of desmosomal deficiency.[20] Furthermore, tomographic electron microscopy (T-EM; *Figure 2* and Supplementary material online, *Video*) revealed that the expanded intercellular space coincided with the presence of membrane invaginations in one side of the intercalated disc. *Figure 2A–F* shows selected planes of the same section, revealing that the invaginations extended several nanometres into the intracellular space; in some planes, the invaginations seemed to 'pinch off', leaving a healed membrane continuum facing the intercellular cleft. This observation was confirmed in three separate samples analysed by T-EM, and not found in controls.[18]

3.2 Sodium current properties in adult ventricular myocytes of PKP2-Hz mice

Previous studies have demonstrated that acute loss of PKP2 expression leads to decreased amplitude and shift in gating and kinetics of the sodium current (I_{Na}).[4] We therefore explored whether a similar effect would be observed in myocytes from PKP2-Hz hearts. As

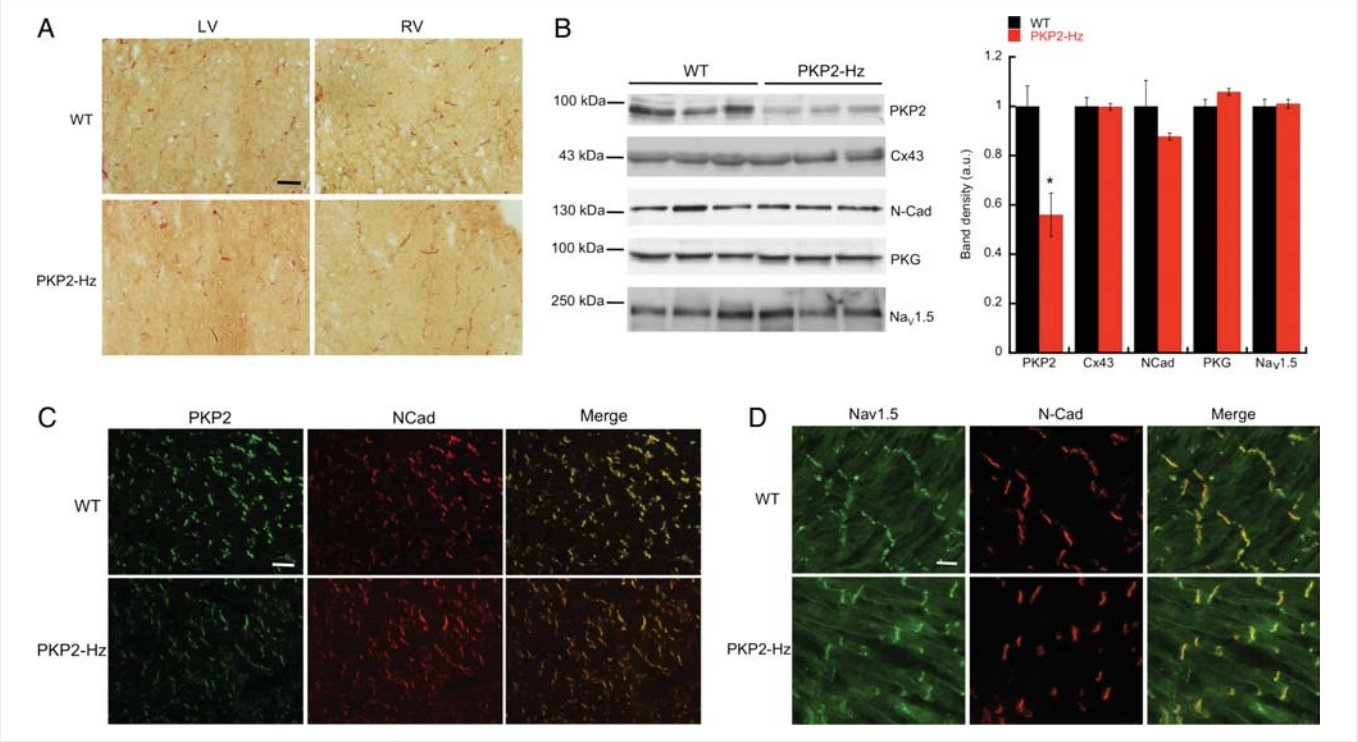

Figure 1 Characterization of PKP2-Hz hearts. (*A*) Picrosirius red staining to determine collagen abundance. Images obtained from left (LV; left) or right ventricle (RV; right) of mice wild type (WT; top) or PKP2-Hz (bottom). Extent of Picrosirius-red staining determined from fraction of Sirius red-positive pixels within a field. Data for each field sampled in a WT heart normalized to average value of 12 random fields in same heart. Data for PKP2-Hz hearts measured relative to average value in littermate WT hearts, processed in parallel. No difference observed between genotypes when compared with respective ventricle: RV-WT: 1.0 ± 0.16, RV-PKP2-Hz: 0.77 ± 0.08; pNS. LV-WT: 1.0 ± 0.15, LV-PKP2-Hz 1.25 ± 0.16; pNS (ANOVA). $N = 4$, $n = 48$. Calibration bar, 50 μm. (*B*) Western blots for intercalated disc proteins. For quantification (right panel), band densities were corrected by total protein, and PKP2-Hz data measured relative to WT on same exposure. *$P < 0.05$ compared with WT. All other comparisons, NS. (*C* and *D*) Immunofluorescence images for PKP2 (green) and N-Cad (red; *C*; Calibration bar, 50 μm) and for $Na_V1.5$ (green) and N-Cad (red; *D*; Calibration bar 25 μm) in WT and PKP2-Hz hearts. No difference was apparent between groups.

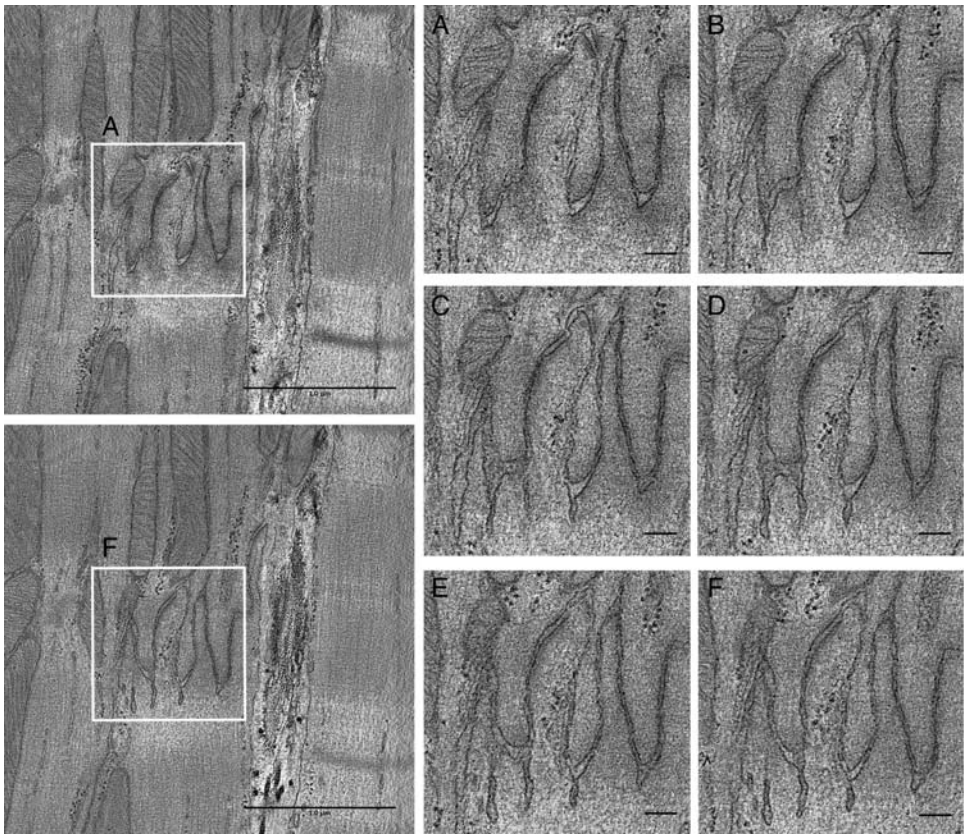

Figure 2 T-EM images of intercalated disc in PKP2-Hz adult heart. Outlined region in left panels, enlarged for insets (*A*–*F*). Each frame corresponding to different plane of visualization. Notice membrane invaginations, extending into the intracellular space and detaching from a healed membrane in some sectional planes.

shown in *Figure 3*, whole-cell patch clamp experiments revealed that average peak sodium current density in PKP2-Hz cells was significantly reduced when compared with control (*Figure 3A*). There was no difference in voltage dependence of activation (*Figure 3B*), but we observed a negative shift in steady-state inactivation (*Figure 3C*), and a slower recovery from inactivation (*Figure 3D*) in cells from PKP2-Hz animals when compared with control. Overall, our studies showed impairment of cardiac sodium current in cells from animals with reduced abundance of PKP2.

3.3 Flecainide-induced decrease in I_{Na} is more pronounced in PKP2-Hz myocytes

Sodium channel blockers such as flecainide can help unveil an—otherwise masked or minimal—sodium current deficit.[7,8,10–12,21] We explored whether the use dependence of flecainide block could be more pronounced in PKP2-Hz cells than in control. *Figure 4A* depicts the time course of average peak I_{Na} density, relative to that at onset of recording, measured by 100 ms voltage clamp steps from −120 to −30 mV applied, repetitively, every 300 ms. Control recordings (no drug) were obtained for 50–60 s after patch break. Flecainide (1 μmol/L) was added to the superfusate at the time indicated by the upward arrow. No voltage clamp steps were applied for the first 3 min after addition of the drug (voltage clamp off; cell at resting membrane potential). After that period, membrane voltage was clamped again and the repetitive pulse protocol reinitiated. The peak current density elicited by the first pulse following quiescence reflected the magnitude of the 'tonic' (as opposed to 'use-dependent') blocking effect of the drug. Subsequent pulses elicited currents of progressively decreasing amplitude, reflecting the use dependence of the flecainide block. The reduction in I_{Na} density was significantly larger in PKP2-Hz cells (red) than in control (black). Compiled data obtained from experiments testing three different flecainide concentrations are shown in *Figure 4B* and *C*. The bar graphs in *Figure 4B* show the extent of use-dependent block, whereas *Figure 4C* compares the time course. The black and red bars represent data from control and PKP2-Hz cells, respectively. The results show that flecainide caused a more pronounced, and faster block in PKP2-Hz cells (Supplementary material online, *Table S1* for numerical parameters).

3.4 Flecainide-induced slow conduction velocity is more pronounced in PKP2-Hz hearts

Additional experiments explored the flecainide effect on electrophysiological parameters recorded by electrical epicardial activation mapping of Langendorff-perfused whole heart preparations. *Figure 5A* shows examples of activation maps from a littermate control (WT; left) and a PKP2-Hz mouse (right), in the absence or presence of 0.53 μmol/L of flecainide (drug concentrations of 1 μmol/L led to the loss of propagated activity in some preparations).

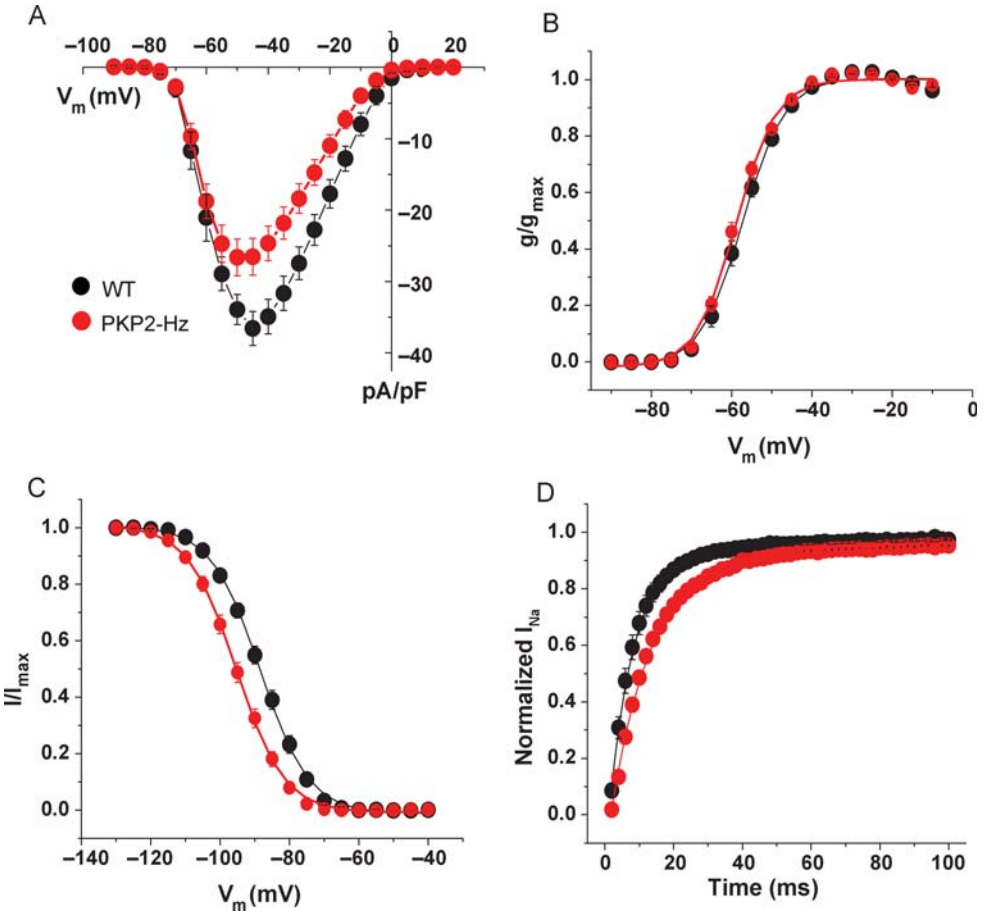

Figure 3 Sodium current properties recorded from adult cardiac myocytes isolated from PKP2-Hz hearts. (*A*) Average peak sodium current density as a function of voltage command. Peak current amplitude at −45 mV: WT: −36.1 ± 2.4 pA/pF; $n = 12$. PKP2-Hz: −26.3 ± 2.6 pA/pF; $n = 16$. $P < 0.01$. (*B*) Voltage dependence of steady-state activation curves. Voltage for half-maximal activation ($V_{1/2}$): −57.4 ± 0.9 mV for WT and −58.9 ± 0.7 mV for PKP2-Hz (pNS). (*C*) Voltage dependence of steady-state inactivation. Voltage for half-maximal inactivation ($V_{1/2}$): −89.6 ± 1.4 mV for WT and −95.3 ± 1.1 mV for PKP2-Hz ($P < 0.005$). (*D*) Time course of recovery from inactivation. Time constant (one exponential function): 8.5 ± 0.9 ms for WT and 11.9 ± 0.7 ms for PKP2-Hz ($P < 0.002$).

The crowding of the isochrones reflects the fact that flecainide caused a decrease in longitudinal propagation velocity, which was most prominent in PKP2-Hz hearts. Cumulative data are shown in Supplementary material online, *Table S2*. Graphs depicting the measurements of longitudinal conduction velocity for right and left ventricles are shown in *Figure 5B* and *C*, respectively. The data show that the flecainide-induced decrease was most prominent for RV propagation along the fibre direction ($P < 0.02$ vs. littermate controls), with the consequent decrease in anisotropic ratio for RV (Supplementary material online, *Table S2*). A similar tendency was observed for left ventricular propagation, although the difference was not statistically significant. Qualitatively, these results were reminiscent of those obtained in SCN5A haplo-insufficient hearts.[22]

3.5 Flecainide-induced electrocardiographic changes and ventricular arrhythmias in PKP2-Hz mice

Our results in isolated cells and whole heart preparations led us to explore genotype-dependent electrocardiographic differences. Single-lead, surface ECGs were recorded from anaesthetized animals. At baseline, PKP2-Hz animals presented significantly longer *P* wave duration; other ECG baseline parameters were similar to control (Supplementary material online, *Table S3*; *Figure 6*). A flecainide challenge (83 μmol/kg i.p.) caused a prolongation of the *P* and QRS durations, and of the PR and QTc intervals. In average, the flecainide effect was significantly more pronounced in PKP2-Hz animals than in control (*Figure 6A*, left panel shows an example; *Figure 6B* and Supplementary material online *Table S4* for cumulative data recorded at baseline, 5′ and 10′). A similar result was obtained when the relative increase in a given variable (as per cent of its magnitude at baseline) was analysed (Supplementary material online, *Figure S3* and Table *S5*). Flecainide also induced second degree AV block in 8/12 PKP2-Hz and 5/11 WT animals. Two out of 12 PKP2-Hz (and 0/11 WT controls) showed atrial arrhythmias. More importantly, 6/12 PKP2-Hz animals showed ventricular arrhythmias, not observed in any of the 11 WT mice tested ($P = 0.01$; *Figure 6A*, right panel for examples of ventricular arrhythmias in PKP2-Hz mice). Arrhythmic death during recording occurred in 3 PKP2-Hz animals; none of the WT died during the procedure.

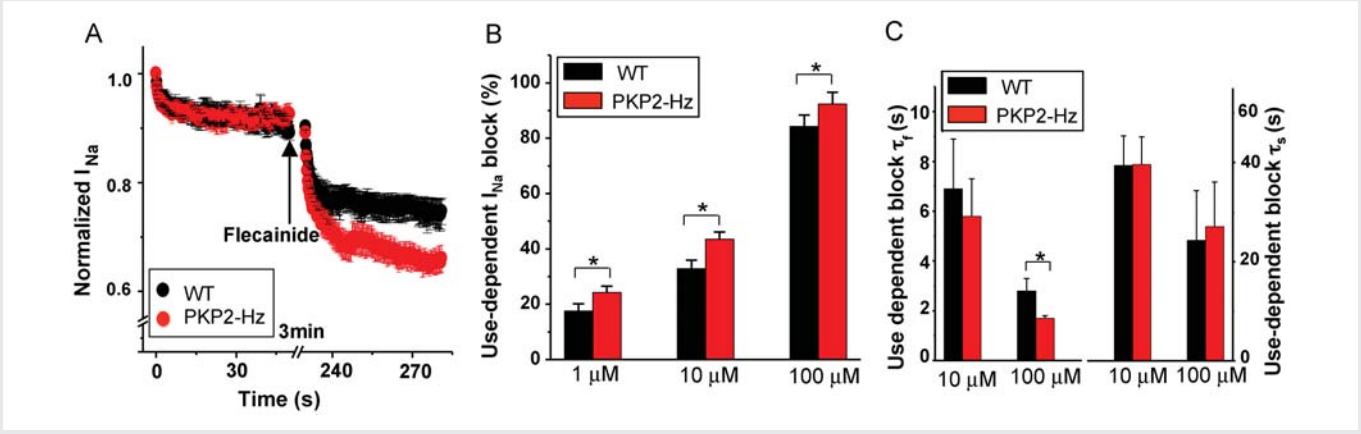

Figure 4 PKP2 deficiency and use-dependent, flecainide-induced I_{Na} block. (*A–C*) Data from adult ventricular myocytes dissociated from either PKP2-Hz (red) or WT littermates (black). (*A*) Time course of I_{Na}, relative to current density at patch break. After 60 s of regular pacing, voltage clamp pulses were interrupted, and Flecainide (1 μmol/L) added (arrow). Repetitive pulses were re-initiated 3 min after addition of drug. SEM noted for each time point. (*B*) Compiled data for fraction of current decrease consequent to use-dependent flecainide block. WT, $n = 8, 9, 8$ and PKP2-Hz $n = 10, 9, 9$ for 1, 10 and 100 μmol/L flecainide, respectively. $^*P < 0.05$ for each concentration. (*C*) Fast and slow time constants of use-dependent flecainide block ($^*P < 0.05$).

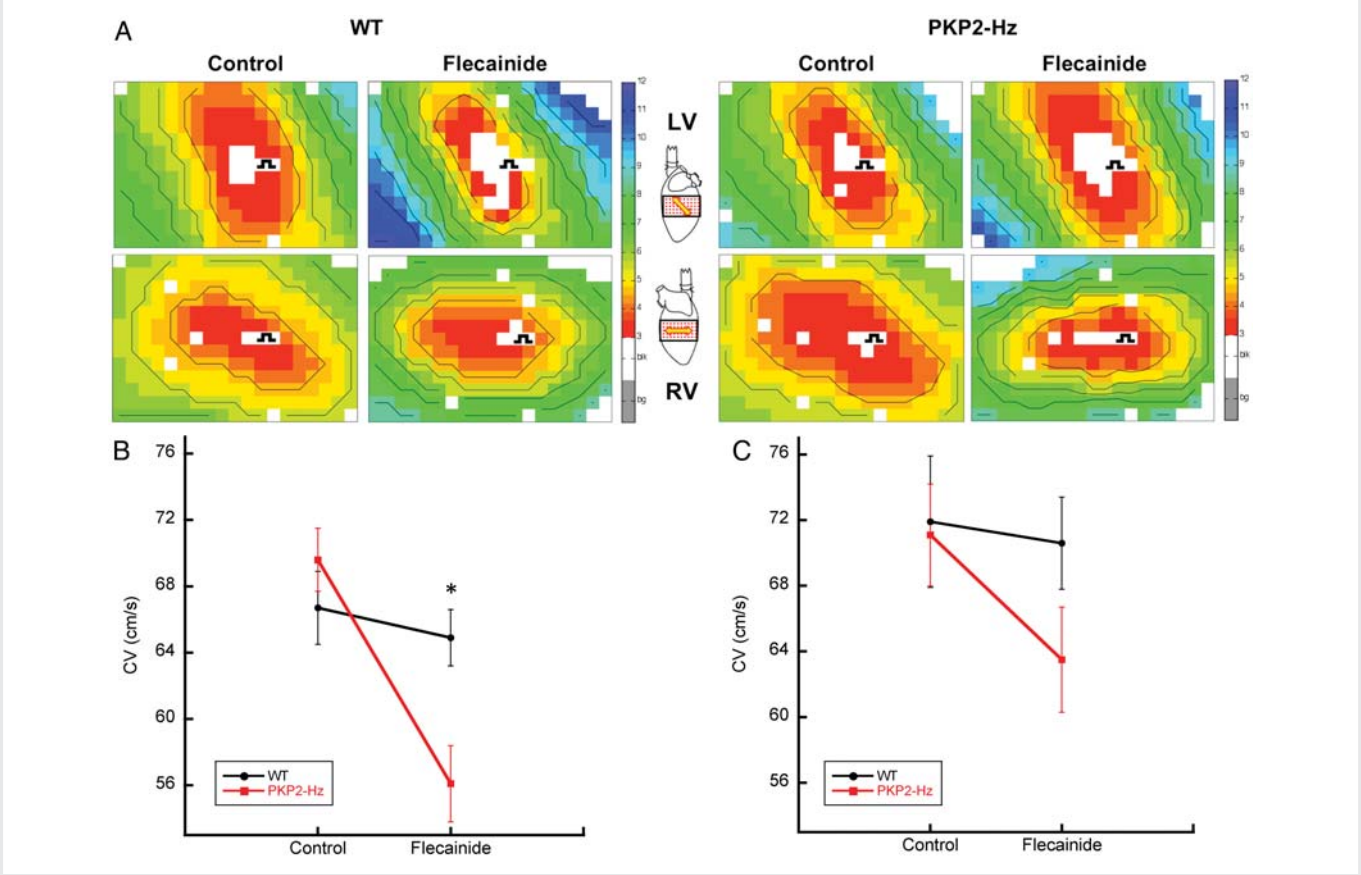

Figure 5. Epicardial activation maps in PKP2-Hz and control hearts. (*A*) Examples of activation maps for left (LV; top) and right ventricle (RV; bottom) of WT (left) and PKP2-Hz hearts in the absence or presence of flecainide. Colours indicate activation times. Isochrones outlined by black lines. Area depicted within each frame: 5.4 by 3.6 mm. Site of stimulation indicated by square-pulse symbol. (*B* and *C*) Average longitudinal conduction velocity (CV), measured in right (RV; *B*) or left ventricle (LV; *C*) of either WT (black symbols) or PKP2-Hz mice (red symbols). $^*P < 0.05$.

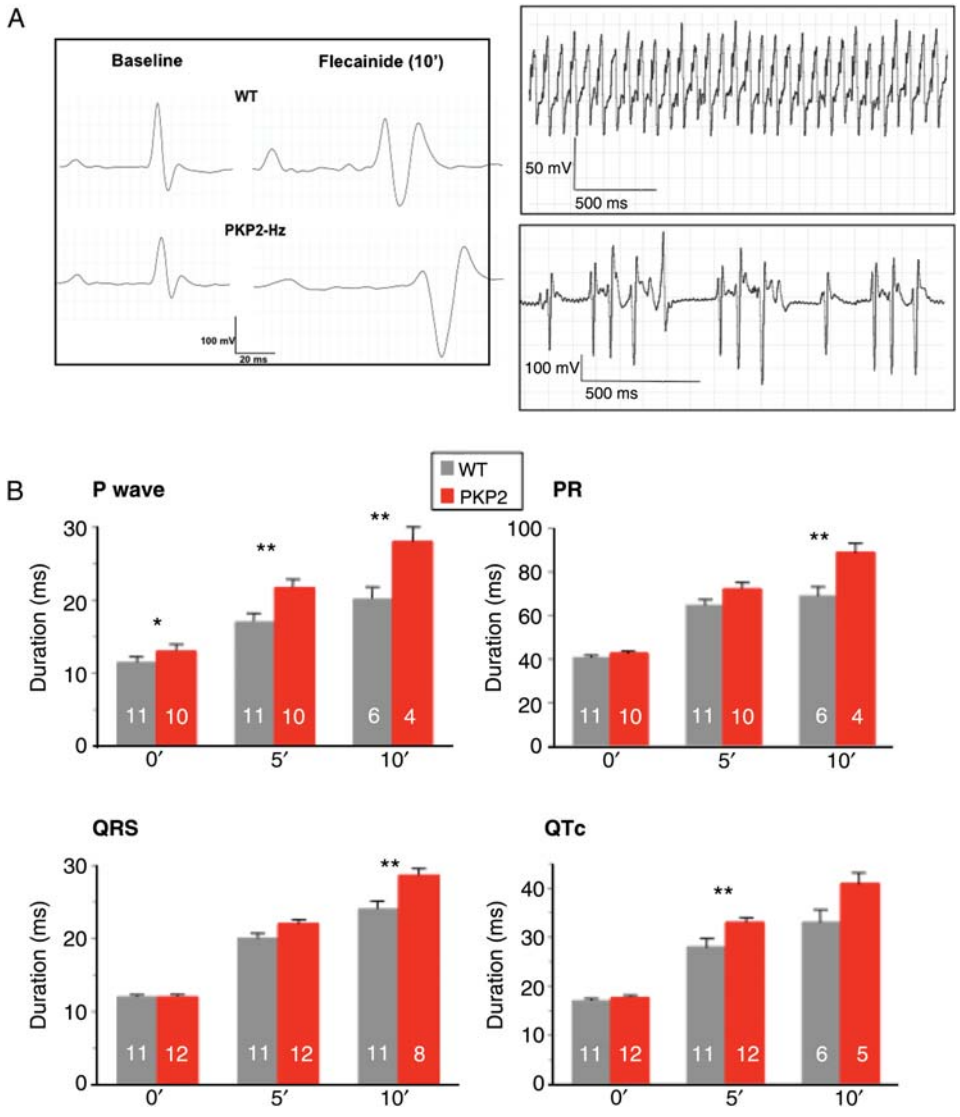

Figure 6. Electrocardiographic features of PKP2-Hz mice at baseline, and in response to flecainide. (*A*) Left, example of ECG traces from WT (top) and PKP2-Hz mouse, (bottom). Recordings obtained at baseline (left) and 10 min after flecainide (40 mg/kg i.p., right). Right: VT in PKP2-Hz mice. Recordings obtained from two animals, 10′ (top) and 9′ (bottom) after flecainide i.p. (*B*) Graph bars show average *P* wave duration, PR interval, QRS duration, and QTc interval measured at baseline, 5′ and 10′ after flecainide injection. A total of 11 WT and 12 PKP2-Hz animals were studied. Criteria for exclusion from data set: for *P* duration and PR interval, subject excluded from data set if ECG showed at least one of the following (number of excluded subjects from a given time point, in parentheses): (1) ventricular tachycardia, VT (4 PKP2-Hz at 10′), (2) second-degree AV block (5 WT, 3 PKP2-Hz at 10′), (3) atrial tachycardia, diagnosed for altered *P* polarity and shorter PR interval (one PKP2-Hz at 5′ and at 10′), or (4) *P* wave inversion, likely signalling a low atrial rhythm (two PKP2-Hz at baseline and at 5′). First two criteria also applied to QTc data set. For QRS duration, animals in VT were excluded; animals in second degree AV block were included, with parameters measured only from conducted sinus beats. *n* values indicated in each bar. $*P < 0.05$; $**P \leq 0.01$. Additional data in Supplementary material online, *Tables S3—S5* and *Figure S3*.

4. Discussion

We have shown that a decrease in PKP2 abundance associates with sodium channel dysfunction in mice. A significant difference in sodium current properties was observed in control (*Figure 3*); the sodium current deficit was amplified by superfusion with flecainide (*Figure 4*). Flecainide also lead to genotype-dependent slowing of longitudinal conduction (*Figure 5*), electrocardiographic changes (*Figure 6*), and increased susceptibility to ventricular arrhythmias and death (*Figure 6*). The electrophysiological phenotype was observed in the absence of overt structural disease (*Figure 1*), although with an ultrastructural phenotype (*Figure 2*). Overall, our data support the notion that a genetically mediated decrease in PKP2 abundance can directly impair the function of the voltage-gated sodium channel complex, and cardiac electrophysiological behaviour, even when structural integrity of the heart is not compromised. Together with our studies on the molecular interactions between PKP2 and components of the voltage-gated sodium channel complex,[3] and all differences between an animal model and a human disease being noted, our data suggest a potential mechanistic insight into the origin of arrhythmias that occur in patients with mutations in the *pkp2* gene and no overt structural disease.

Yet, sodium current may not be the only affected variable. Further studies will be necessary to determine whether junctional conductance, amplitude/kinetics of repolarizing currents, and/or extent of electrical heterogeneity are affected by the loss of PKP2 in a manner similar to what has been observed after the loss of other junctional molecules.[18,23–25]

Flecainide has primary effects as a use-dependent sodium channel blocker, and our results further found a genotype-dependent effect (*Figure 4*). Both flecainide and PKP2 deficiency lead to slow recovery from I_{Na} inactivation.[4,26] We therefore speculate that the combination of both factors leads to a more extensive impairment of I_{Na} during repetitive activation. Based on the results on isolated cells, we further speculate that the flecainide-induced changes in conduction velocity (*Figure 5* and Supplementary material online, *Table S2*) were primarily consequent to sodium current deficit. We also observed that flecainide had a more pronounced effect on conduction velocity in the right ventricle (*Figure 5B*). This is consistent with other studies showing that sodium current deficit leads to preferential impairment of propagation in the right ventricle.[27,28] The mechanism for this effect is unknown, although it has been speculated that it relates to the fact that the RV-free wall is thinner, and it also shows sharp shifts in fibre orientation across the wall. The larger layer-to-layer rotational anisotropy may be associated with poor electrical coupling, slower conduction, and preferential sites for conduction block.[29,30] Moreover, the right-vs.-left heterogeneity may have facilitated the initiation, and maintenance of ventricular arrhythmias *in vivo* (*Figure 6*). The heterogeneous distribution of the sodium channel protein in the conduction system and across the ventricular wall may have also contributed to arrhythmogenesis.[27] Our results are also consistent with *in silico* studies demonstrating that PKP2-dependent changes in I_{Na} can lead to initiation and sustainment of vortex activity.[31] It should be noted, however, that flecainide also has effects on other currents;[32–35] moreover, disruption of the area composita (see our *Figure 2*) may affect potassium channels.[25] Whether PKP2 deficiency also affects other ion currents, and their response to flecainide treatment, remains to be determined. The experimental data, however, point to the sodium current deficit as a primary mechanism for the observed effects.

A deficiency in PKP2 abundance has been associated with various cases of familial AC.[5] It has been suggested that arrhythmias in patients with AC are consequent to reentrant activity around anatomical obstacles. While such a mechanism is certainly possible, life-threatening ventricular arrhythmias or sudden death often occur in the concealed phase of the disease, prior to overt structural damage.[5] The intimate mechanisms responsible for these arrhythmias are less clear. Decreased gap junction-mediated electrical coupling could be an adjuvant to arrhythmogenesis, although it is unlikely to be the only cause.[22,36,37] Obvious differences between animal models and clinical cases notwithstanding the data presented in this study support the notion that patients with haploinsufficiency in the *pkp2* gene (mutation R79x, for example; see ref.[38,39]) may present a sodium current deficit. As in the case of the PKP2-Hz mice, this deficit may remain masked, but could be unveiled by an external trigger. In that regard, it is important to note that hearts from patients that have succumbed to ventricular fibrillation often reveal the presence of inflammatory infiltrates. Separate studies have revealed elevated levels of serum inflammatory mediators, and myocardial expression of IL-17 and TNF-alpha, in patients with AC.[40] Previous data suggest that cytokines can alter sodium current function.[41,42] Future studies will address whether PKP2 is involved in modulating the response of I_{Na} to cytokines, in a manner that would facilitate the loss of the cardiac rhythm in the setting of an inflammatory response in a PKP2-deficient heart.

It is interesting to note that, as opposed to other animal models of desmosomal deficiency, PKP2-Hz mice do not develop a structural disease. The reason as to why decreased *pkp2* gene dose and decreased PKP2 protein do not lead to the structural manifestations of AC in mice is unclear; yet, the observation is consistent with the limited penetrance of the structural disease,[5,43] and supports the idea that epigenetic factors (e.g. an inflammatory response[40]) perhaps not present in the 'sterile' environment of the laboratory animals, may be necessary to trigger fibrofatty infiltration. On the other hand, the model allows to study arrhythmogenic substrates related to PKP2 deficiency in the absence of structural involvement, a feature particularly helpful to understand the electrical phenotype of the desmosome-deficient heart in the concealed phase of the disease.

The present study focused on the phenotype of PKP2-Hz hearts. Whether other desmosomal proteins also interact with $Na_V1.5$, and whether these interactions occur in human heart, is currently under investigation. Recently, Gomes *et al.*[44] reported that desmoplakin-heterozygous mice present average peak sodium current density similar to control; yet, careful analysis of their results suggests the possibility of technical limitations in their voltage clamp recordings, which could have masked small differences between the groups (see timing of peak current in the traces at the bottom of their *Figure 1F*, left-shift in Vm for peak current in the IV plot, and overall shape of IV curve; experiments carried out at $[Na]o = 25$ mM; $[Na]i = 5$ mM with patch electrodes of 3–4 MΩ); moreover, gating and kinetic properties were not thoroughly studied. On the other hand, patients with heterozygous mutations in desmoplakin and without overt structural disease showed significant regional conduction delays and heterogeneous $Na_V1.5$ distribution.[44] In summary, there is new evidence in support of the hypothesis, first proposed by our laboratory,[4] that I_{Na} is affected by desmosomal mutations. Additional studies are necessary to better understand this interaction. Furthermore, characterizing the role of I_{Na} in desmosome disease will be important as guidance on the indication or contraindication of sodium channel blockers in patients affected with AC. Finally, sodium channel blockers (including flecainide) are used as diagnostic tools in humans suspect of Brugada syndrome, a disease often associated with primary deficiency in sodium channel function.[9] Whether flecainide would aid in the evaluation of the arrhythmia risk in patients suspect of AC is an interesting area that deserves further investigation.

Supplementary material

Supplementary material is available at *Cardiovascular Research* online.

Acknowledgements

We acknowledge the support of the Electron Microscopy Core (Office of Collaborative Science) of New York University Langone Medical Center for electron microscopy services, and NYSBC for high-pressure freezing and electron tomography data collection.

Conflict of interest: none declared.

Funding

This work was supported by grants from National Institute of Health HL106632 and HL087226 (M.D.), HL084583, HL083422 (P.M.); a Foundation Leducq Transatlantic Network (M.D.), the Netherlands Heart Foundation grant 2007B139, and the Interuniversity Cardiology Institute of the Netherlands; project #06901.

References

1. Petitprez S, Zmoos AF, Ogrodnik J, Balse E, Raad N, El-Haou S *et al*. Sap97 and dystrophin macromolecular complexes determine two pools of cardiac sodium channels Nav1.5 in cardiomyocytes. *Circ Res* 2011;**108**:294–304.
2. Malhotra JD, Thyagarajan V, Chen C, Isom LL. Tyrosine-phosphorylated and nonphosphorylated sodium channel beta1 subunits are differentially localized in cardiac myocytes. *J Biol Chem* 2004;**279**:40748–40754.
3. Sato PY, Coombs W, Lin X, Nekrasova O, Green KJ, Isom LL *et al*. Interactions between ankyrin-G, plakophilin-2, and connexin43 at the cardiac intercalated disc. *Circ Res* 2011;**109**:193–201.
4. Sato PY, Musa H, Coombs W, Guerrero-Serna G, Patino GA, Taffet SM *et al*. Loss of plakophilin-2 expression leads to decreased sodium current and slower conduction velocity in cultured cardiac myocytes. *Circ Res* 2009;**105**:523–526.
5. Delmar M, McKenna WJ. The cardiac desmosome and arrhythmogenic cardiomyopathies: from gene to disease. *Circ Res* 2010;**107**:700–714.
6. Grossmann KS, Grund C, Huelsken J, Behrend M, Erdmann B, Franke WW *et al*. Requirement of plakophilin 2 for heart morphogenesis and cardiac junction formation. *J Cell Biol* 2004;**167**:149–160.
7. Martin CA, Guzadhur L, Grace AA, Lei M, Huang CL. Mapping of reentrant spontaneous polymorphic ventricular tachycardia in a SCN5a+/− mouse model. *Am J Physiol Heart Circ Physiol* 2011;**300**:H1853–H1862.
8. Stokoe KS, Balasubramaniam R, Goddard CA, Colledge WH, Grace AA, Huang CL. Effects of flecainide and quinidine on arrhythmogenic properties of SCN5a+/− murine hearts modelling the Brugada syndrome. *J Physiol* 2007;**581**:255–275.
9. Meregalli PG, Ruijter JM, Hofman N, Bezzina CR, Wilde AA, Tan HL. Diagnostic value of flecainide testing in unmasking SCN5a-related Brugada syndrome. *J Cardiovasc Electrophysiol* 2006;**17**:857–864.
10. Scicluna BP, Tanck MW, Remme CA, Beekman L, Coronel R, Wilde AA *et al*. Quantitative trait loci for electrocardiographic parameters and arrhythmia in the mouse. *J Mol Cell Cardiol* 2011;**50**:380–389.
11. Antzelevitch C, Brugada P, Borggrefe M, Brugada J, Brugada R, Corrado D *et al*. Brugada syndrome: report of the second consensus conference: endorsed by the heart rhythm society and the European heart rhythm association. *Circulation* 2005;**111**:659–670.
12. Brugada R, Brugada J, Antzelevitch C, Kirsch GE, Potenza D, Towbin JA *et al*. Sodium channel blockers identify risk for sudden death in patients with ST-segment elevation and right bundle branch block but structurally normal hearts. *Circulation* 2000;**101**:510–515.
13. van Rijen HV, van Veen TA, van Kempen MJ, Wilms-Schopman FJ, Potse M, Krueger O *et al*. Impaired conduction in the bundle branches of mouse hearts lacking the gap junction protein connexin40. *Circulation* 2001;**103**:1591–1598.
14. van Rijen HV, Eckardt D, Degen J, Theis M, Ott T, Willecke K *et al*. Slow conduction and enhanced anisotropy increase the propensity for ventricular tachyarrhythmias in adult mice with induced deletion of connexin43. *Circulation* 2004;**109**:1048–1055.
15. Potse M, Linnenbank AC, Grimbergen CA. Software design for analysis of multichannel intracardial and body surface electrocardiograms. *Comput Methods Programs Biomed* 2002;**69**:225–236.
16. Martin CA, Zhang Y, Grace AA, Huang CL. In vivo studies of SCN5a+/− mice modeling Brugada syndrome demonstrate both conduction and repolarization abnormalities. *J Electrocardiol* 2010;**43**:433–439.
17. Delmar M, Liang FX. Connexin43 and the regulation of intercalated disc function. *Heart Rhythm* 2012;**9**:835–838.
18. Jansen JA, Noorman M, Musa H, Stein M, de Jong S, van der Nagel R *et al*. Reduced heterogeneous expression of Cx43 results in decreased Nav1.5 expression and reduced sodium current that accounts for arrhythmia vulnerability in conditional Cx43 knockout mice. *Heart Rhythm* 2012;**9**:600–607.
19. Hund TJ, Koval OM, Li J, Wright PJ, Qian L, Snyder JS *et al*. A beta(iv)-spectrin/CAMKII signaling complex is essential for membrane excitability in mice. *J Clin Invest* 2010;**120**:3508–3519.
20. Kant S, Krull P, Eisner S, Leube RE, Krusche CA. Histological and ultrastructural abnormalities in murine desmoglein 2-mutant hearts. *Cell Tissue Res* 2012;**348**:249–259.
21. Leoni AL, Gavillet B, Rougier JS, Marionneau C, Probst V, Le Scouarnec S *et al*. Variable Na(v)1.5 protein expression from the wild-type allele correlates with the penetrance of cardiac conduction disease in the SCN5a(+/−) mouse model. *PLoS ONE* 2010;**5**:e9298.
22. Stein M, van Veen TA, Hauer RN, de Bakker JM, van Rijen HV. A 50% reduction of excitability but not of intercellular coupling affects conduction velocity restitution and activation delay in the mouse heart. *PLoS ONE* 2011;**6**:e20310.
23. Oxford EM, Musa H, Maass K, Coombs W, Taffet SM, Delmar M. Connexin43 remodeling caused by inhibition of plakophilin-2 expression in cardiac cells. *Circ Res* 2007;**101**:703–711.
24. Danik SB, Rosner G, Lader J, Gutstein DE, Fishman GI, Morley GE. Electrical remodeling contributes to complex tachyarrhythmias in connexin43-deficient mouse hearts. *FASEB J* 2008;**22**:1204–1212.
25. Cheng L, Yung A, Covarrubias M, Radice GL. Cortactin is required for n-cadherin regulation of kv1.5 channel function. *J Biol Chem* 2011;**286**:20478–20489.
26. Ramos E, O'Leary ME. State-dependent trapping of flecainide in the cardiac sodium channel. *J Physiol* 2004;**560**:37–49.
27. Remme CA, Verkerk AO, Hoogaars WM, Aanhaanen WT, Scicluna BP, Annink C *et al*. The cardiac sodium channel displays differential distribution in the conduction system and transmural heterogeneity in the murine ventricular myocardium. *Basic Res Cardiol* 2009;**104**:511–522.
28. van Veen TA, Stein M, Royer A, Le Quang K, Charpentier F, Colledge WH *et al*. Impaired impulse propagation in scn5a-knockout mice: combined contribution of excitability, connexin expression, and tissue architecture in relation to aging. *Circulation* 2005;**112**:1927–1935.
29. Schalij MJ, Boersma L, Huijberts M, Allessie MA. Anisotropic reentry in a perfused 2-dimensional layer of rabbit ventricular myocardium. *Circulation* 2000;**102**:2650–2658.
30. Vetter FJ, Simons SB, Mironov S, Hyatt CJ, Pertsov AM. Epicardial fiber organization in swine right ventricle and its impact on propagation. *Circ Res* 2005;**96**:244–251.
31. Deo M, Sato PY, Musa H, Lin X, Pandit SV, Delmar M *et al*. Relative contribution of changes in sodium current versus intercellular coupling on reentry initiation in 2-dimensional preparations of plakophilin-2-deficient cardiac cells. *Heart Rhythm* 2011;**8**:1740–1748.
32. Du CY, El Harchi A, Zhang YH, Orchard CH, Hancox JC. Pharmacological inhibition of the HERG potassium channel is modulated by extracellular but not intracellular acidosis. *J Cardiovasc Electrophysiol* 2011;**22**:1163–1170.
33. Caballero R, Dolz-Gaiton P, Gomez R, Amoros I, Barana A, Gonzalez de la Fuente M *et al*. Flecainide increases Kir2.1 currents by interacting with cysteine 311, decreasing the polyamine-induced rectification. *Proc Natl Acad Sci USA* 2010;**107**:15631–15636.
34. Radicke S, Vaquero M, Caballero R, Gomez R, Nunez L, Tamargo J *et al*. Effects of mirp1 and dpp6 beta-subunits on the blockade induced by flecainide of Kv4.3/Kchip2 channels. *Br J Pharmacol* 2008;**154**:774–786.
35. Akar FG, Wu RC, Deschenes I, Armoundas AA, Piacentino V 3rd, Houser SR *et al*. Phenotypic differences in transient outward K+ current of human and canine ventricular myocytes: insights into molecular composition of ventricular Ito. *Am J Physiol Heart Circ Physiol* 2004;**286**:H602–H609.
36. Danik SB, Liu F, Zhang J, Suk HJ, Morley GE, Fishman GI *et al*. Modulation of cardiac gap junction expression and arrhythmic susceptibility. *Circ Res* 2004;**95**:1035–1041.
37. Gutstein DE, Morley GE, Tamaddon H, Vaidya D, Schneider MD, Chen J *et al*. Conduction slowing and sudden arrhythmic death in mice with cardiac-restricted inactivation of connexin43. *Circ Res* 2001;**88**:333–339.
38. van Tintelen JP, Entius MM, Bhuiyan ZA, Jongbloed R, Wiesfeld AC, Wilde AA *et al*. Plakophilin-2 mutations are the major determinant of familial arrhythmogenic right ventricular dysplasia/cardiomyopathy. *Circulation* 2006;**113**:1650–1658.
39. van der Zwaag PA, Cox MG, van der Werf C, Wiesfeld AC, Jongbloed JD, Dooijes D *et al*. Recurrent and founder mutations in the Netherlands: plakophilin-2 p.Arg79x mutation causing arrhythmogenic right ventricular cardiomyopathy/dysplasia. *Neth Heart J* 2010;**18**:583–591.
40. Asimaki A, Tandri H, Duffy ER, Winterfield JR, Mackey-Bojack S, Picken MM *et al*. Altered desmosomal proteins in granulomatous myocarditis and potential pathogenic links to arrhythmogenic right ventricular cardiomyopathy. *Circ Arrhythm Electrophysiol* 2011;**4**:743–752.
41. Grandy SA, Brouillette J, Fiset C. Reduction of ventricular sodium current in a mouse model of HIV. *J Cardiovasc Electrophysiol* 2010;**21**:916–922.
42. Lin X, Liu N, Lu J, Zhang J, Anumonwo JM, Isom LL *et al*. *Subcellular* heterogeneity of sodium current properties in adult cardiac ventricular myocytes. *Heart Rhythm* 2011;**8**:1923–1930.
43. Gerull B, Heuser A, Wichter T, Paul M, Basson CT, McDermott DA *et al*. Mutations in the desmosomal protein plakophilin-2 are common in arrhythmogenic right ventricular cardiomyopathy. *Nat Genet* 2004;**36**:1162–1164.
44. Gomes J, Finlay M, Ahmed AK, Ciaccio EJ, Asimaki A, Saffitz JE *et al*. Electrophysiological abnormalities precede overt structural changes in arrhythmogenic right ventricular cardiomyopathy due to mutations in desmoplakin-a combined murine and human study. *Eur Heart J*. Advance Access publication January 11, 2012, doi:10.1093/eurheartj/ehr472.